

**Understanding the Effect of the Dianhydride Structure on the Properties of Semi-aromatic Polyimides
Containing a Biobased Fatty Diamine**

Arijana Susa^{†*}, Johan Bijleveld[†], Marianella Hernandez Santana^{†‡}, Santiago J. Garcia[†]

[†] Novel Aerospace Materials group, Faculty of Aerospace Engineering
Delft University of Technology, Kluyverweg 1, 2629 HS, Delft, The Netherlands

[‡] Currently at Institute of Polymer Science and Technology (ICTP-CSIC)
Juan de la Cierva, 3, 28006, Madrid, Spain

**e-mail: a.susa@tudelft.nl*

Number of Pages: 10 (S1 to S10)

Number of Figures: 8

Number of Tables: 1

List of figures and tables:

Page No.:

Figure S1.	¹ H NMR spectra of the four polymers in CDCl ₃ and their assignment to the molecular structure.	S2 – S4
Figure S2.	TGA curves showing weight loss with temperature of the four PIs in the as synthesized state.	S5
Figure S3.	DSC traces of the second heating curves, showing glass transitions of the four PIs in the as synthesized state.	S5
Figure S4.	Normalized dielectric loss (ϵ'') of PI samples with different dianhydrides at selected temperatures (25, 40, 50 and 70 °C).	S6
Figure S5.	Temperature dependence of the average relaxation time for the segmental mode of PIs.	S7
Figure S6.	Arrhenius plots of the time-temperature superposition shift factors a_T for the glass transition relaxations of the four PIs.	S8
Table S1.	Activation energies for the glass transition relaxations.	S8
Figure S7.	Polarized microscopy images of the BPDA-D polymer showing the increase in birefringence with annealing time.	S9
Figure S8.	SAXS diffractograms of BPDA-D polymer showing the annealing effect on the structural ordering.	S10

Yield

Percent yield of the polymer was calculated according to equation:

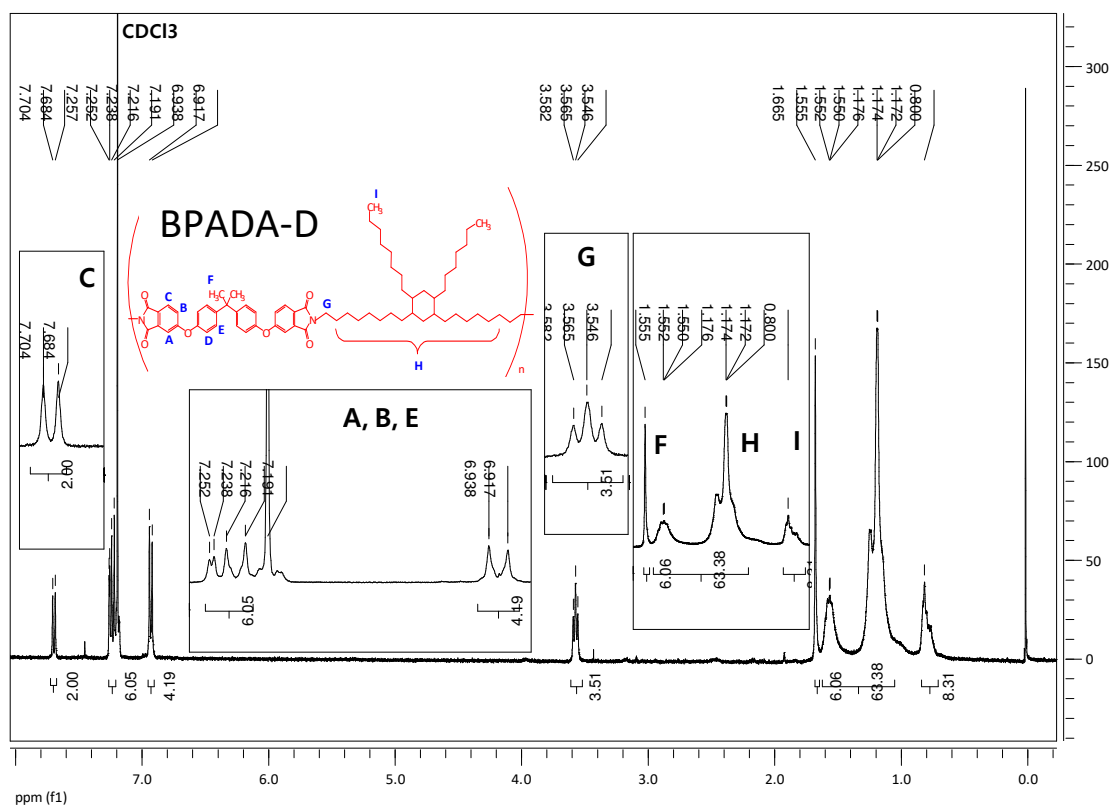
$$\text{Percent yield (\%)} = 100 \left(\frac{\text{Actual mass of the product}}{\text{Predicted mass of the product}} \right) \quad (\text{Eq. S1})$$

where predicted mass of the product was calculated according to the stoichiometric balance, assuming that 1 mol of a dianhydride (DAh) and 1 mol of DD1 give 1 mol of PI and 2 mol of water (4.25 wt% of water):

$$\text{Predicted mass of the product/g} = m(\text{DAh}) + m(\text{DD1}) - m(\text{H}_2\text{O}) \quad (\text{Eq. S2})$$

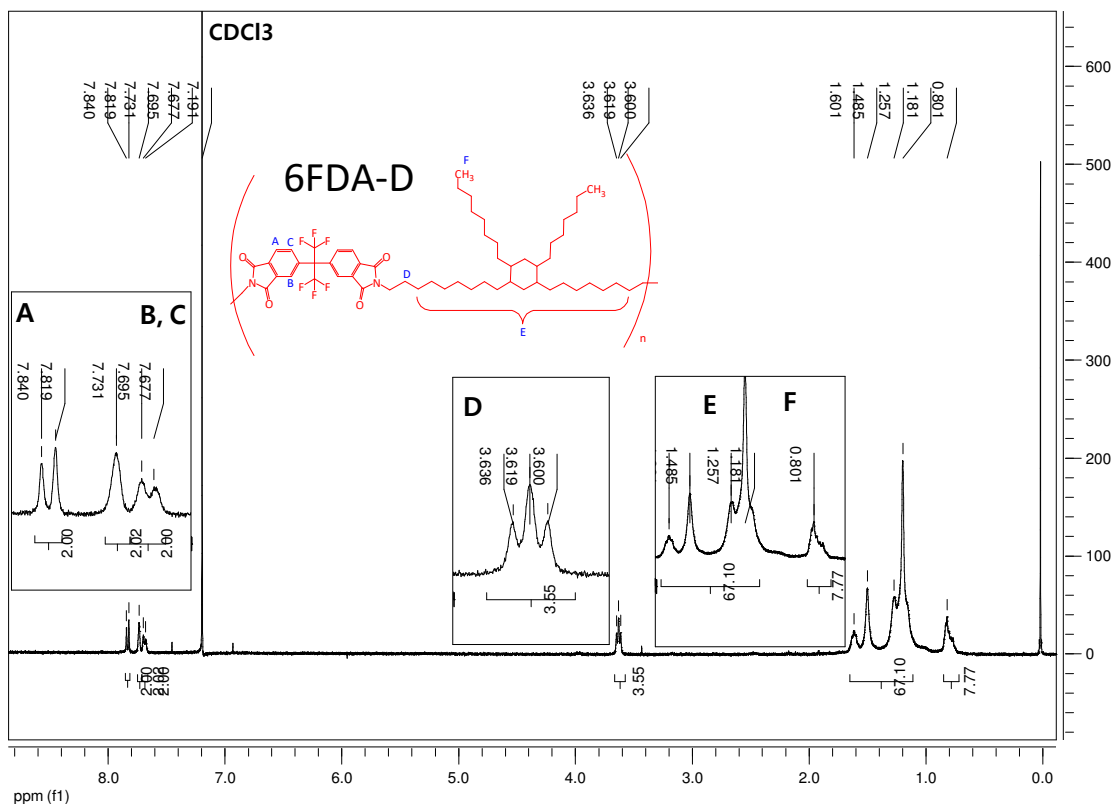
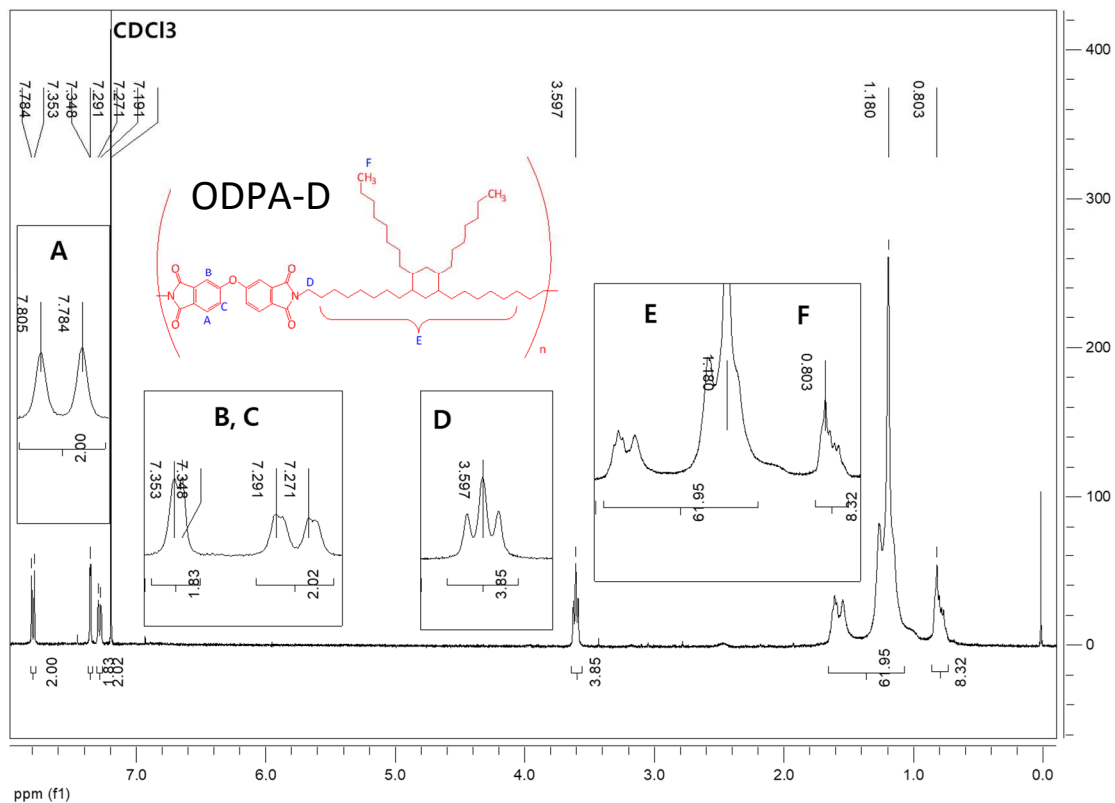
¹H NMR spectra

Solution state ¹H NMR spectra were collected using the Agilent-400 MR DD2 at 25°C at 400 MHz. The solutions of polymers were prepared in CDCl₃. Spectra were referenced to the solvent residual peak for TMS. Spectra were not normalized.



SUPPORTING INFORMATION

Susa et al. 2017



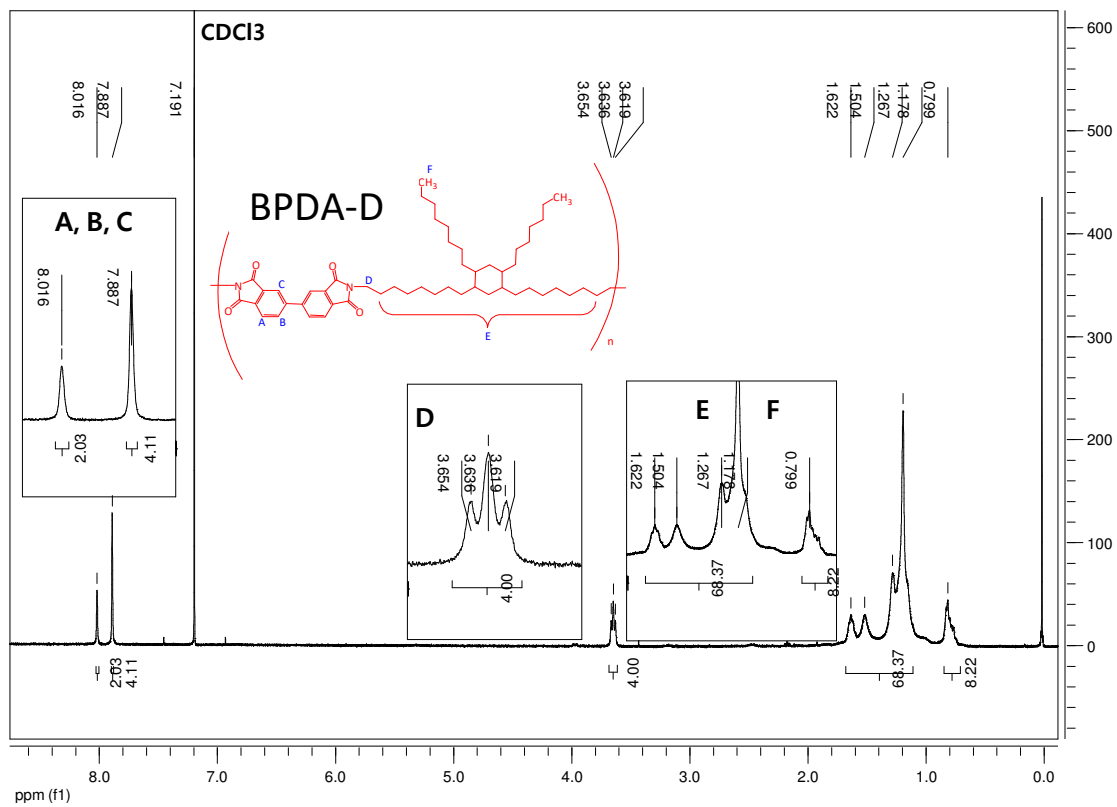


Figure S1. ¹H NMR spectra of the four polymers in CDCl₃ and their assignment to the molecular structure.

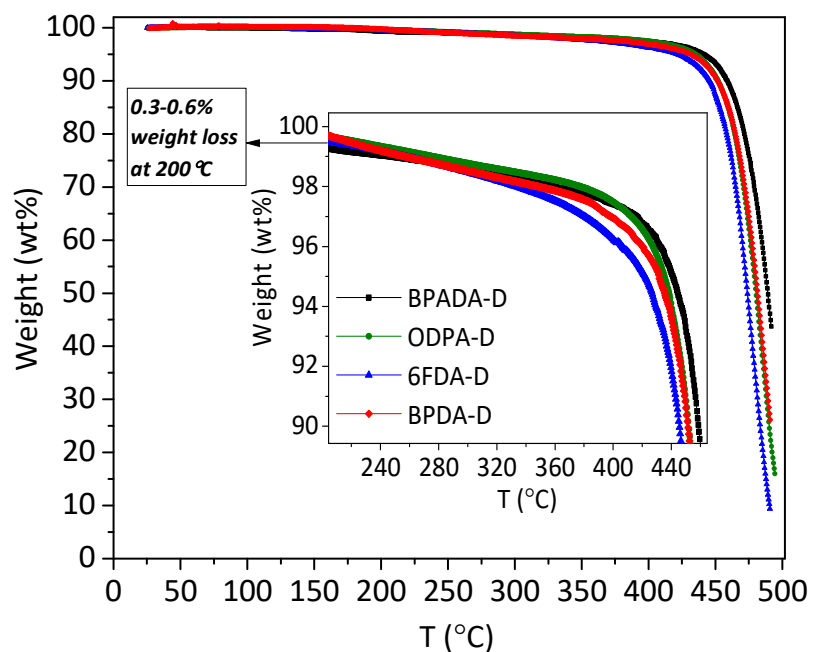


Figure S2. TGA curves showing weight loss (wt%) with temperature of the four PIs in the as synthesized state.

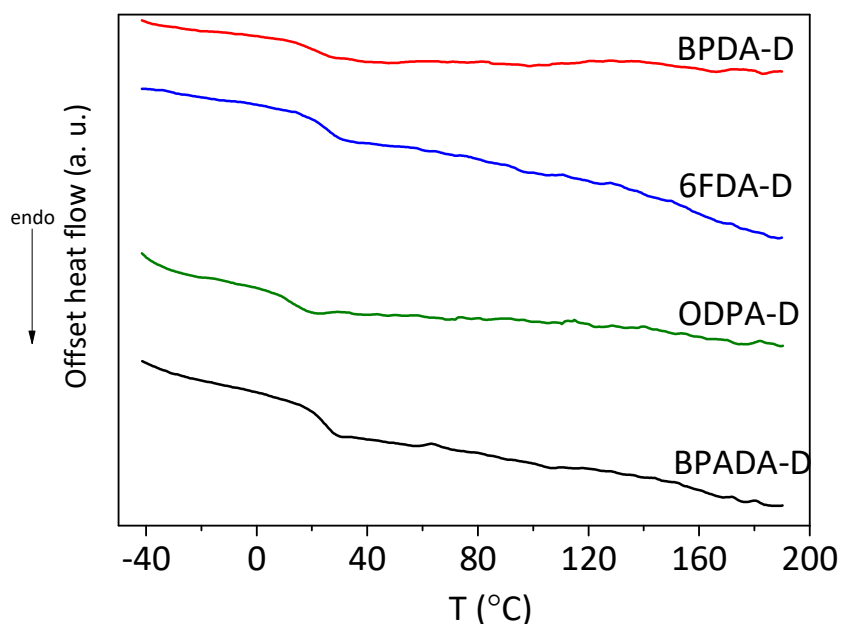


Figure S3. DSC traces of the second heating curves, showing glass transitions of the four PIs in the as synthesized state.

Broadband dielectric spectroscopy (BDS) analysis

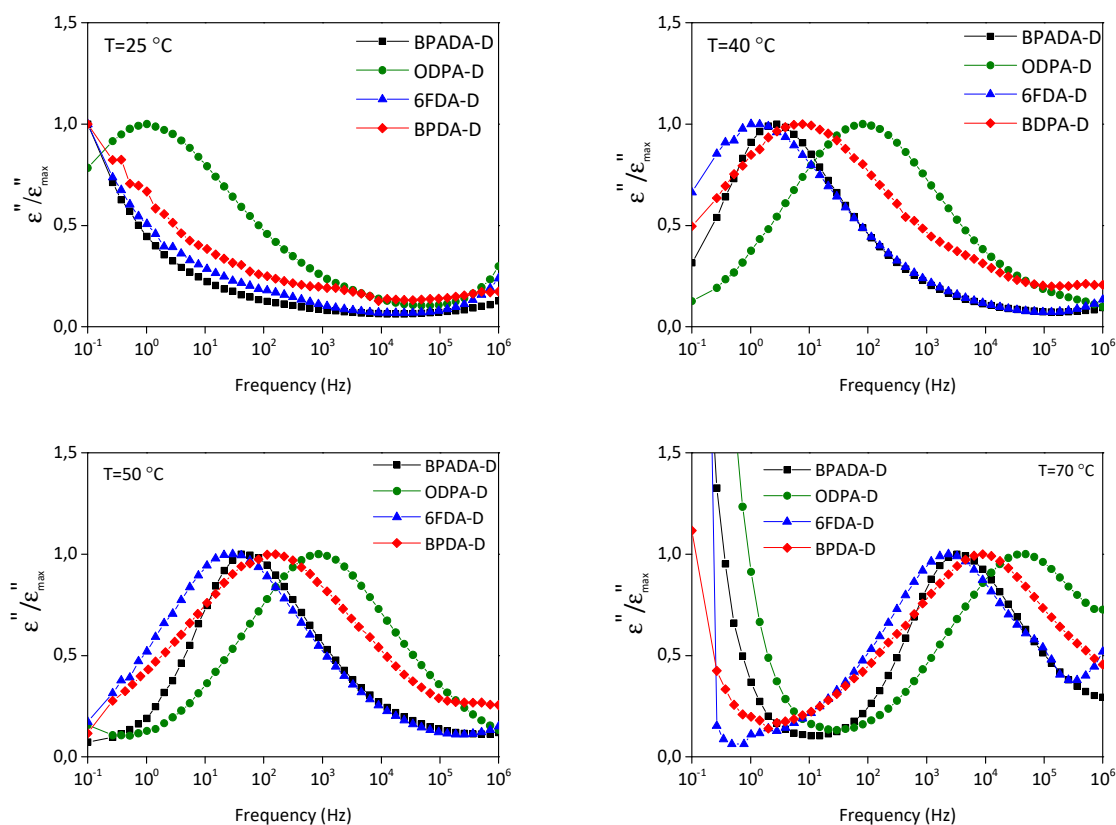


Figure S4. Normalized dielectric loss (ϵ'') of PI samples with different dianhydrides at selected temperatures (25 , 40, 50 and 70 °C).

The dielectric relaxation processes were analyzed quantitatively by fitting the frequency spectra to the Havriliak-Negami (HN) function^{1,2} given by:

$$\epsilon^*(\omega) = \epsilon_{\infty} + \frac{\Delta\epsilon}{[1+(i\omega\tau_{HN})^b]^c} \quad (\text{Eq.S3})$$

The difference in dielectric constant measured at low and high frequencies is the *dielectric strength* ($\Delta\epsilon$) of the relaxation and it is related to the area under the absorption curve given by ($\Delta\epsilon = \epsilon_s - \epsilon_{\infty}$), where ϵ_{∞} and ϵ_s are the unrelaxed and relaxed values of the dielectric constant respectively. τ_{HN} is the HN relaxation time, representing the most probable relaxation time of the relaxation time distribution function,³ and b and c are shape parameters ($0 < b, c \leq 1$) which describe the symmetric and the asymmetric broadening of the equivalent relaxation time distribution function, respectively. Parameters b and c can be associated to the structure and polymer architecture heterogeneity with respect to the bulk polymer.

The HN relaxation time τ_{HN} is related to the frequency of maximum loss, $f_{\max} = 1/(2\pi\tau_{\max})$, by the following equation:⁴

$$\tau_{\max} = \frac{1}{2\pi f_{\max}} = \tau_{\text{HN}} \left(\sin \frac{b\pi}{2+2c} \right)^{-1/b} \left(\sin \frac{bc\pi}{2+2c} \right)^{1/b} \quad (\text{Eq. S4})$$

Both characteristic relaxation times coincide when the relaxation spectrum is symmetric, *i.e.* $c=1$.

The temperature dependence of the segmental relaxation times (τ_{\max}) was also studied. This dependency is well stated by the Vogel-Fulcher-Tammann (VFT) equation:⁵⁻⁸

$$\tau_{\max} = \tau_0 \exp \left(\frac{B}{T-T_0} \right) \quad (\text{Eq. S5})$$

where τ_0 and B are temperature-independent parameters, and T_0 is the so-called ideal glass transition or Vogel temperature which is found to be 30-70 K below T_g .⁹ To reduce the effect of misleading parameters on data fitting to the VFT equation over a limited frequency range, a value of $\tau_0 \approx 10^{-14}$ s was assumed, according to the values empirically found for many polymer systems lying between 10^{-14} and 10^{-12} . The dependence of τ_{\max} with temperature is depicted in Figure S5. This temperature dependency shows a clear curvature typical for cooperative motions.

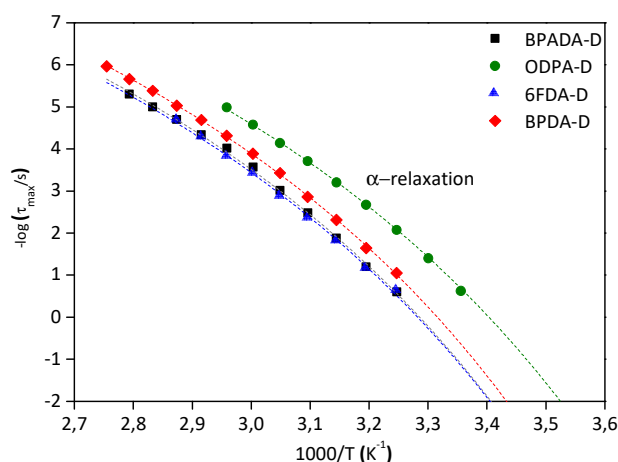


Figure S5. Temperature dependence of the average relaxation time for the segmental mode of PIs. Dotted lines correspond to the VFT fit.

¹ Kremer, F.; Schönhal, A., *Broadband Dielectric Spectroscopy*. Springer: New York, **2003**; p 721.

² Havriliak, S.; Negami, S., A Complex Plane Representation of Dielectric and Mechanical Relaxation Processes in Some Polymers. *Polymer* **1967**, *8* (4), 161-210. DOI: 10.1016/0032-3861(67)90021-3

³ Böttcher, C. J. F.; Bordewijk, P., *Theory of Electric Polarization*. Elsevier: **1978**; Vol. II.

⁴ Richert, R.; Angell, C. A., Dynamics of Glass-forming Liquids. V. On the Link Between Molecular Dynamics and Configurational Entropy. *J Chem Phys* **1998**, *108* (21), 9016-9026. DOI: 10.1063/1.476348

⁵ Fulcher, G. S., Analysis of Recent Measurements of the Viscosity of Glasses. *J Am Ceram Soc* **1925**, *8* (6), 339-355. DOI: 10.1111/j.1151-2916.1925.tb16731.x

⁶ Vogel, H., The Temperature Dependence Law of the Viscosity of Fluids. *Physikalische Zeitschrift* **1921**, *22*, 645-646.

⁷ Tammann, G.; Hesse, W., The Dependency of Viscosity on Temperature in Hypothermic Liquids. *Zeitschrift Fur Anorganische Und Allgemeine Chemie* **1926**, *156* (4).

⁸ Bohmer, R.; Ngai, K. L.; Angell, C. A.; Plazek, D. J., Nonexponential Relaxations in Strong and Fragile Glass Formers. *J Chem Phys* **1993**, *99* (5), 4201-4209. DOI: 10.1063/1.466117

⁹ Fischer, E. W., Light-scattering and Dielectric Studies on Glass-forming Liquids. *Physica A* **1993**, *201* (1-3), 183-206. DOI: 10.1016/0378-4371(93)90416-2

Activation energies for the glass transition relaxations

From the shift factors obtained from the TTS mastercurves, the Arrhenius plots ($\ln a_T$ vs $1000/T$) were constructed and the activation energies were calculated from the slopes of the linear fit according to the Arrhenius equation:¹⁰

$$a_T = \exp\left[\frac{E_a}{R}\left(\frac{1}{T} - \frac{1}{T_{ref}}\right)\right] \quad (\text{Eq. S6})$$

Where a_T is the shift factor, E_a is the activation energy, R is the gas constant and T_{ref} is the reference temperature at which the mastercurve is constructed.

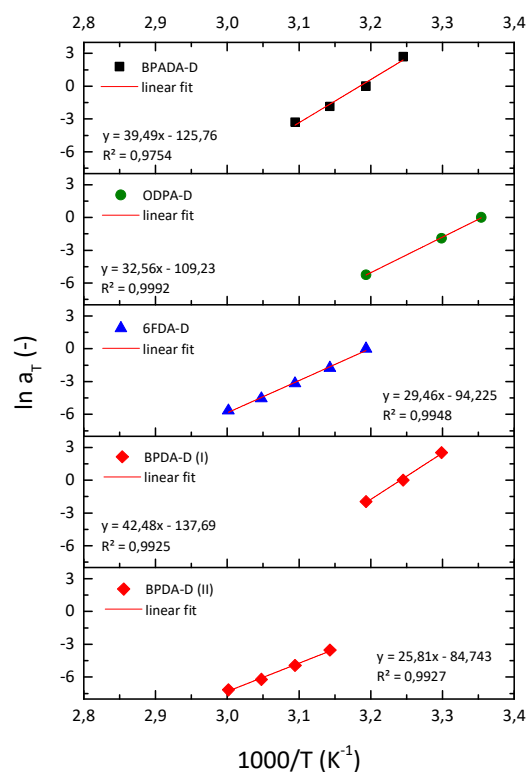


Figure S6. Arrhenius plots of the time-temperature superposition shift factors a_T for the glass transition relaxations of the four PIs. Note that BPADA-D shows two T_g relaxations (I and II) while the other three polymers show only one.

$$T_{ref} = T(\tan \delta_{MAX}) = T_g.$$

Table S1. Activation energies for the glass transition relaxations

Polymer	Relaxation process	E_a / kJmol^{-1}
BPADA-D	T_g	328
ODPA-D	T_g	271
6FDA-D	T_g	245
BPADA-D	T_g (I)	353
	T_g (II)	215

¹⁰ Wood-Adams, P.; Costeux, S., Thermorheological Behavior of Polyethylene: Effects of Microstructure and Long Chain Branching. *Macromolecules* **2001**, *34* (18), 6281-6290. DOI: 10.1021/ma0017034

Birefringence with annealing time

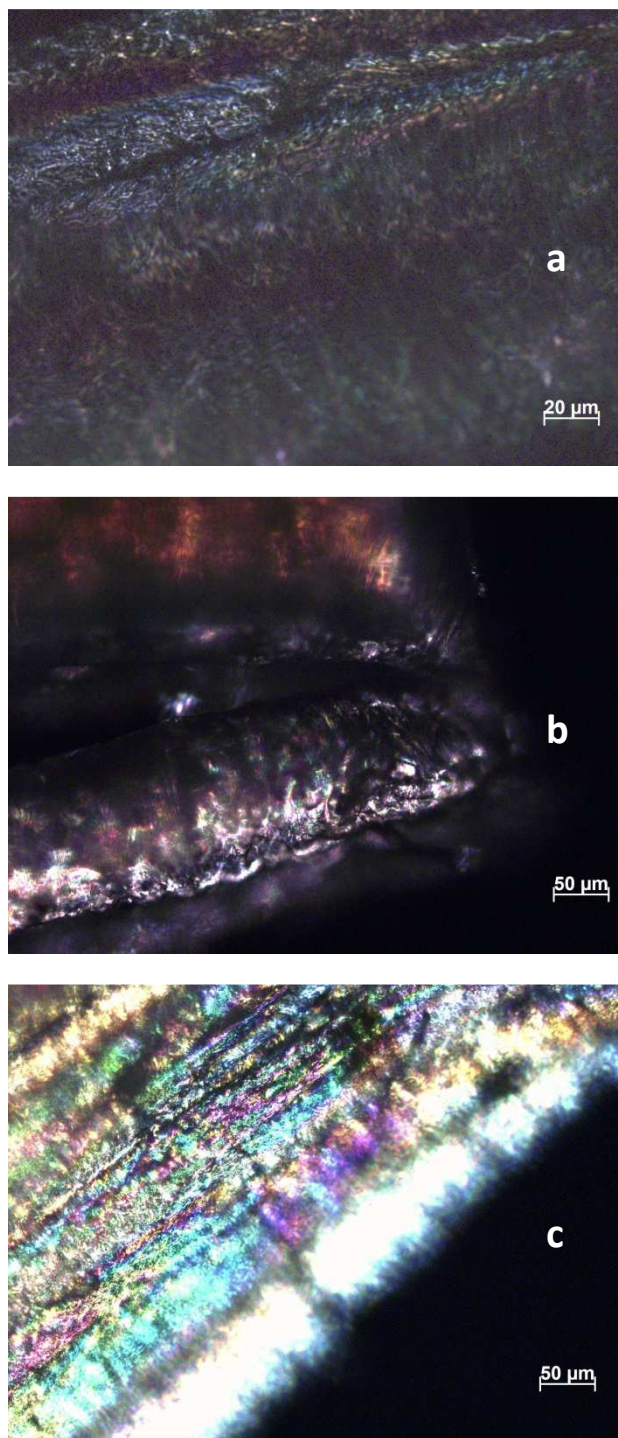


Figure S7. Polarized microscopy images of the BPDA-D polymer showing the increase in birefringence with annealing time for a) non-annealed, b) 5 days annealed and c) 11 days annealed samples.

SAXS measurements

The SAXS diffractograms were collected using Anton Paar SAXSess, with a copper tube operated at 40 mA, 40 kV, using a multilayer mirror for focusing and monochromatisation of the emitted X-ray beam. The detector is a Dectris Mythen photon counting strip detector. The samples have been measured for 20 minutes each, with the sample mounted on a holder in vacuum. The data was corrected for dark-current, transmission and a background (empty holder subtracted). The data was subsequently desmeared using a procedure available in the SAXSQuant software. The data was then regrouped or rebinned to reduce the number of datapoints and noise, taking care to propagate the uncertainties. The separation distances, d , are calculated according to $d=2\pi/q$.¹¹

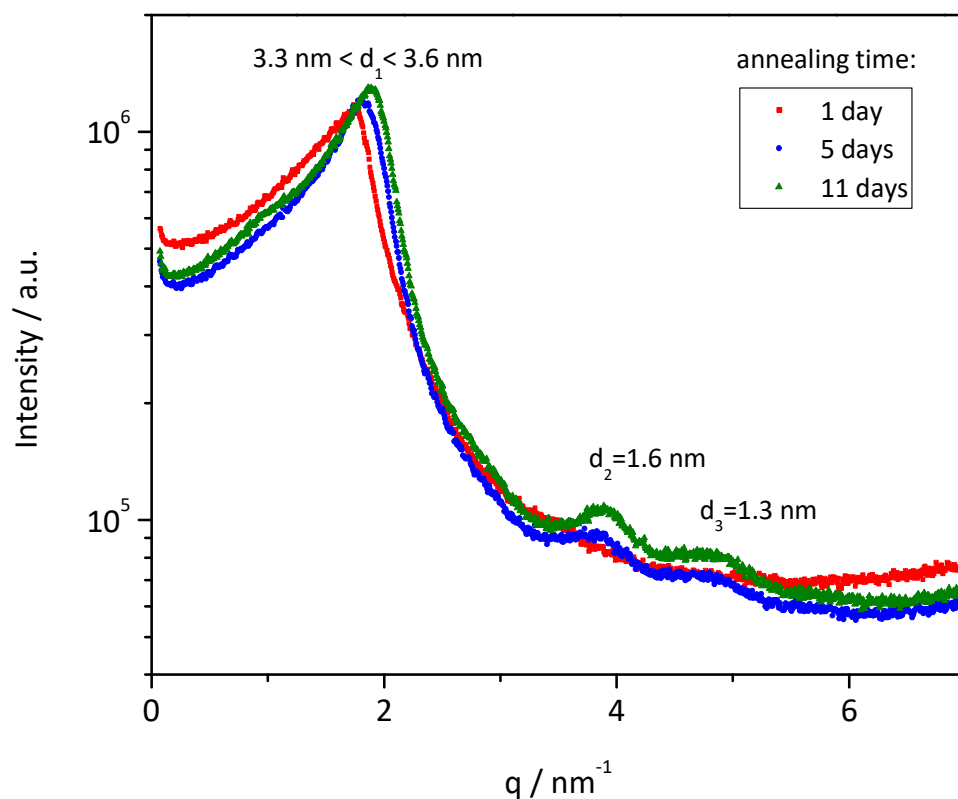


Figure S8. SAXS diffractograms of BPDA-D polymer that was annealed at $T_{\text{ann}}=T(\tan \delta_{\text{MAX}})=T_g$ for different times: 1 day (red squares), 5 days (blue circles) and 11 days (green triangles). The annealed samples show two additional peaks that indicate nanophase separation. The calculated separation distances, d , are assigned to each peak.

¹¹ Beiner, M.; Huth, H., Nanophase Separation and Hindered Glass Transition in Side-chain Polymers. *Nat Mater* **2003**, 2 (9), 595-599. DOI: 10.1038/nmat966